Available online at www.sciencedirect.com
SCIENCE DIRECT
Coastal Engineering 53 (2006) 311 – 318
Coastal Engineering
An International Journal for Coastal, Harbour and Offshore Engineers
www.elsevier.com/locate/coastaleng

Comparison of time-dependent extended mild-slope equations for random waves

Changhoon Lee [a,*], Gunwoo Kim [b], Kyung-Duck Suh [c]

[a] Department of Civil and Environmental Engineering, Sejong University, 98 Kunja-Dong, Kwangjin-Gu, Seoul 143-747, South Korea
[b] School of Civil, Urban, and Geosystem Engineering, Seoul National University, San 56-1, Shinlim-Dong, Gwanak-Gu, Seoul 151-742, South Korea
[c] School of Civil, Urban, and Geosystem Engineering and Engineering Research Institute, Seoul National University, San 56-1, Shinlim-Dong, Gwanak-Gu, Seoul 151-742, South Korea

Received 23 August 2004; received in revised form 20 April 2005; accepted 10 August 2005
Available online 20 December 2005

Abstract

The extended mild-slope equations of Suh et al. [Suh, K.D., Lee, C., Park, W.S., 1997. Time-dependent equations for wave propagation on rapidly varying topography. Coastal Eng., 32, 91–117] and Lee et al. [Lee, C., Kim, G., Suh, K.D., 2003. Extended mild-slope equation for random waves. Coastal Eng., 48, 277–287] are compared analytically and numerically to determine their applicability to random wave transformation. The geometric optics approach is used to compare the two models analytically. In the model of Suh et al., the wave number of the component wave with a local angular frequency ω is approximated with an accuracy of $O(\omega-\bar{\omega})$ at a constant water depth, where $\bar{\omega}$ is the carrier frequency of random waves. In the model of Suh et al., however, the diffraction effects and higher-order bottom effects are considered only for monochromatic waves, and the shoaling coefficient of random waves is not accurately approximated. This inaccuracy arises because the model of Suh et al. was derived for regular waves. In the model of Lee et al., all the parameters of random waves such as wave number, shoaling coefficient, diffraction effects, and higher-order bottom effects are approximated with an accuracy of $O(\omega-\bar{\omega})$. This approximation is because the model of Lee et al. was developed using the Taylor series expansion technique for random waves. The result of dispersion relation analysis suggests the use of the peak and weighted-average frequencies as a carrier frequency for Suh et al. and Lee et al. models, respectively. All the analytical results are verified by numerical experiments of shoaling of random waves over a slightly inclined bed and diffraction of random waves through a breakwater gap on a flat bottom.

Keywords: Numerical model; Extended mild-slope equation; Water waves; Random wave transformation

1. Introduction

Since the development of a mild-slope equation by Berkhoff (1972), many coastal engineers have developed wave models to analyze the combined refraction and diffraction of water waves. In order to predict the propagation of random waves with a narrow frequency band, time-dependent mild-slope equations were developed. A time-dependent mild-slope equation was developed by Smith and Sprinks (1975) using the Green's formula. A canonical form of the time-dependent mild-slope equations was developed by Radder and Dingemans (1985) using the Hamiltonian theory of surface waves. Another type of time-dependent mild-slope equation was developed by Kubo et al. (1992) using the Taylor series expansion technique for waves with local frequencies different from the carrier frequency. Lee and Kirby (1994) analyzed the mild-slope equations developed by Smith and Sprinks and Kubo et al. in terms of the dispersion relation and energy transport. Considering the dispersion relation, Smith and Sprinks' model was found to be more accurate for analysis in shallower water ($kh \leq 0.2\pi$), where k is the wave number and h is the still water depth, whereas the model of Kubo et al. was more accurate in deeper water ($kh > 0.2\pi$). Considering the energy transport, the model of Kubo et al. was more accurate but has a singularity problem in the higher frequency ranges.

Nishimura et al. (1983) developed hyperbolic mild-slope equations by vertically integrating the continuity and momentum equations for linear waves. Starting from the time-

* Corresponding author. Fax: +82 2 3408 3332.
E-mail addresses: clee@sejong.ac.kr (C. Lee), maossi1@snu.ac.kr (G. Kim), kdsuh@snu.ac.kr (K.-D. Suh).

0378-3839/$ - see front matter © 2005 Elsevier B.V. All rights reserved.
doi:10.1016/j.coastaleng.2005.08.002

dependent mild-slope equation of Smith and Sprinks, Copeland (1985) developed similar hyperbolic equations using the characteristics of linear waves and the associated volume flux. These two hyperbolic equation models predict the transformation of regular waves.

The mild-slope equations were derived based on the assumption of $|\nabla h|/kh \ll 1$ (where ∇ is the horizontal gradient operator) to neglect the terms of the second-order bottom effect such as bottom curvature and squared bottom slope. To account for the effect of rapidly varying bottom topography, Massel (1993) and Chamberlain and Porter (1995) derived the extended mild-slope equations using the Galerkin-eigenfunction method. Chandrasekera and Cheung (1997) provided an alternative derivation of the extended equation using the approach of Berkhoff (1972). Suh et al. (1997) used the Green's second identity and Lagrangian formula to develop two ultimately equivalent hyperbolic equations for random waves. Lee et al. (1998) recast the elliptic formulation of Massel into a hyperbolic formulation, following the technique of Copeland (1985). More recently, Lee et al. (2003) developed another type of time-dependent extended mild-slope equation for random waves, following the technique of Kubo et al. (1992).

There are two methods to predict the transformation of random waves using the time-dependent mild-slope equations. The first method is to superpose the solutions of wave energy which are calculated in more than scores of frequency components by the models for either regular or multi-directional random waves. The second method is to directly predict the transformation of multi-directional random waves by the models for random waves using the coefficients such as $\bar{k}$ and $\bar{C}$ which are the wave number and the phase speed, respectively, for the carrier angular frequency $\bar{\omega}$. Generally, the first method of superposition needs higher-loaded computational efforts such as a large disk memory and a long CPU time compared to the second method. Even for random waves with a broad frequency band, the second method needs lower-loaded computational efforts because accurate results can be obtained by dividing the frequency range into a few bands and modeling each of them with a representative carrier frequency. The model of Suh et al. (1997) has been used to predict accurately the transmission of broad-banded random waves over a ripple patch by superposing three solutions with narrow frequency bands. It was also proved that Radder and Dingemans' (1985) model can directly simulate the transformation of multi-directional random waves (Lee and Suh, 1998).

For regular waves, the equations of Suh et al. (1997) and Lee et al. (2003) show the same accuracy in terms of the higher-order bottom effects. The two equations, however, have not been compared yet for random waves. In this study, the two models are compared for random waves by analytical methods and numerical simulations. First, the dispersion relation and the shoaling coefficient corresponding to random waves are compared. Second, the shoaling of random waves over a slightly inclined bed is tested. Third, the diffraction of random waves with a local frequency different from the carrier one is tested. Finally, conclusions are presented.

2. Dispersion relations and shoaling coefficients of the models

2.1. Governing equations

The extended mild-slope equations of Suh et al. (1997) are given by

$$\frac{\partial \eta}{\partial t} = -\nabla\cdot\left(\frac{\overline{C}\,\overline{C}_g}{g}\nabla\tilde{\phi}\right) + \frac{\overline{\omega}^2 - \overline{k}^2\overline{C}\,\overline{C}_g}{g}\tilde{\phi} + \frac{\overline{\omega}^2}{g}\left\{\overline{R}_1(\nabla h)^2 + \overline{R}_2\nabla^2 h\right\}\tilde{\phi} \tag{1}$$

$$\frac{\partial \tilde{\phi}}{\partial t} = -g\eta \tag{2}$$

where η is the surface elevation, $\bar{C}$ and $\bar{C}_g$ are the phase speed and the group velocity, respectively, g is the gravitational acceleration, the over bar indicates the variables associated with the carrier angular frequency $\bar{\omega}$, and $\tilde{\phi}$ is the velocity potential at mean water level, which is related to the velocity potential ϕ by

$$\phi = \frac{\cosh\bar{k}(h+z)}{\cosh\bar{k}h}\tilde{\phi} \tag{3}$$

In Eq. (1), the coefficients $\bar{R}_1$ and $\bar{R}_2$ are related to higher-order bottom effects, which are functions of the water depth and carrier angular frequency (Suh et al., 1997). When $\bar{R}_1=\bar{R}_2=0$, Eqs. (1) and (2) reduce to the equations of Radder and Dingemans (1985).

The equation of Lee et al. (2003) is given by

$$\nabla\cdot\left(\overline{C}\,\overline{C}_g\nabla\hat{\eta}\right) + \left\{\overline{k}^2\overline{C}\,\overline{C}_g + g\bar{u}_1\nabla^2 h + g\bar{u}_2(\nabla h)^2\right\}\hat{\eta} + i\nabla\cdot\left\{\overline{\frac{\partial\left(CC_g\right)}{\partial\omega}}\nabla\frac{\partial\hat{\eta}}{\partial t}\right\} + i\left\{\overline{\frac{\partial\left(k^2CC_g\right)}{\partial\omega}} + g\overline{\frac{\partial u_1}{\partial\omega}}\nabla^2 h + g\overline{\frac{\partial u_2}{\partial\omega}}(\nabla h)^2\right\}\frac{\partial\hat{\eta}}{\partial t} = 0 \tag{4}$$

where $\hat{\eta}$ is related to η by $\eta=\hat{\eta}\exp(-i\bar{\omega}t)$, $i=\sqrt{-1}$, and the coefficients $\bar{u}_1$ and $\bar{u}_2$ are related to higher-order bottom effects, which are functions of the water depth and carrier angular frequency. When $\bar{u}_1=\bar{u}_2=0$, Eq. (4) reduces to the equation of Kubo et al. (1992). The higher-order bottom effects of $\bar{\omega}^2\bar{R}_1$ and $\bar{\omega}^2\bar{R}_2$ in Eq. (1) are mathematically equivalent to $-g\bar{u}_2$ and $-g\bar{u}_1$, respectively, in Eq. (4).

2.2. Eikonal equation and energy transport equation

The geometric optics approach to the governing equation yields the eikonal equation and the transport equation for wave energy, and further, the dispersion relation and the shoaling coefficients can be obtained from the eikonal equation and the transport equation, respectively. In order to get the eikonal equation and transport equation for the models of Suh et al. and Lee et al., we use the same approach as Lee and Kirby (1994).

Combining Eqs. (1) and (2) of Suh et al. in terms of $\tilde{\phi}$ and using the relation of $\partial\tilde{\phi}/\partial t = -g\eta$ give the following equation:

$$\frac{\partial^2\eta}{\partial t^2} - \nabla\cdot\left(\overline{C}\overline{C}_g\nabla\eta\right) + \left(\overline{\omega}^2 - \overline{k}^2\overline{C}\overline{C}_g\right)\eta + \overline{\omega}^2\left(\overline{R}_1(\nabla h)^2 + \overline{R}_2\nabla^2 h\right)\eta = 0 \tag{5}$$

The surface elevation may be defined as

$$\eta = a(x,y)\exp(i\psi) \tag{6}$$

where $a(x,y)$ is the complex amplitude and ψ is the phase function. The phase function ψ has the following relations with the local wave number vector $\mathbf{k}$ and angular frequency ω:

$$\mathbf{k} = \nabla\psi, \quad \omega = -\frac{\partial\psi}{\partial t} \tag{7}$$

Substituting Eq. (6) into Eq. (5) of Suh et al., the real part yields the eikonal equation given by

$$\left(\frac{k}{\overline{k}}\right)^2 = 1 + \frac{\overline{C}}{\overline{C}_g}\left[\left(\frac{\omega}{\overline{\omega}}\right)^2 - 1\right] + \frac{\nabla\cdot\left(\overline{C}\overline{C}_g\nabla a\right)}{\overline{k}^2\overline{C}\overline{C}_g a} - \frac{\overline{C}}{\overline{C}_g}\left[\overline{R}_1(\nabla h)^2 + \overline{R}_2\nabla^2 h\right] \tag{8}$$

The third and last groups of terms in the right hand of Eq. (8) mean the diffraction effect and higher-order bottom effects, respectively. These effects are considered only for monochromatic waves with the carrier angular frequency $\bar{\omega}$ because all of these terms have over bars. Neglecting these terms yields the dispersion relation as

$$\frac{k}{\overline{k}} = \sqrt{1 + \frac{\overline{C}}{\overline{C}_g}\left[\left(\frac{\omega}{\overline{\omega}}\right)^2 - 1\right]} \tag{9}$$

For monochromatic waves with a carrier frequency, the model exactly satisfies the dispersion relation of the linear Stokes waves. For waves with a local frequency different from the carrier one, the dispersion relation of the model is approximate to an accuracy of $O(\omega-\bar{\omega})$. Substituting Eq. (6) into Eq. (5) of Suh et al., the imaginary part yields the energy transport equation given by

$$\nabla\cdot\left(k\overline{C}\overline{C}_g a^2\right) = 0 \tag{10}$$

The shoaling coefficient is obtained from Eq. (10) as

$$K_s = \frac{a}{a_0} = \sqrt{\frac{\left(k\overline{C}\overline{C}_g\right)_0}{k\overline{C}\overline{C}_g}} \tag{11}$$

where the subscript 0 denotes the reference point and the wave number k is determined by the eikonal Eq. (8). For monochromatic waves with a carrier angular frequency, the shoaling coefficient of the model of Suh et al. is equal to the shoaling coefficient of the linear Stokes waves. For random waves with a local angular frequency different from the carrier frequency, the wave number k in the shoaling coefficient of the model of Suh et al. is approximate to an accuracy of $O(\omega-\bar{\omega})$, but the phase velocity $\bar{C}$ and group velocity $\bar{C}_g$ in the shoaling coefficient are not approximate to this accuracy.

The function $\hat{\eta}$ in Eq. (4) of Lee et al. may be defined as

$$\hat{\eta} = a(x,y)\exp[i(\psi+\overline{\omega}t)] \tag{12}$$

Substituting Eq. (12) into Eq. (4) of Lee et al., the real part gives the eikonal equation given by

$$\left(\frac{k}{\overline{k}}\right)^2 = 1 + \frac{1}{1+(\omega-\overline{\omega})\frac{\overline{\frac{\partial}{\partial\omega}\left(CC_g\right)}}{\overline{C}\overline{C}_g}}\left\langle \frac{2(\omega-\overline{\omega})}{\overline{k}\overline{C}_g} + \frac{\nabla\cdot\left\{\left[\overline{C}\overline{C}_g + (\omega-\overline{\omega})\overline{\frac{\partial}{\partial\omega}\left(CC_g\right)}\right]\nabla a\right\}}{\overline{k}^2\overline{C}\overline{C}_g a} + \frac{g}{\overline{k}^2\overline{C}\overline{C}_g} \times \left[\left(\overline{u}_1 + (\omega-\overline{\omega})\overline{\frac{\partial u_1}{\partial\omega}}\right)\nabla^2 h + \left(\overline{u}_2 + (\omega-\overline{\omega}) \times \overline{\frac{\partial u_2}{\partial\omega}}\right)(\nabla h)^2\right]\right\rangle \tag{13}$$

The second and third groups of terms in the angle bracket represent the diffraction effects and higher-order bottom effects, respectively. For monochromatic waves, these effects are exact. For random waves, these effects are approximate to an accuracy of $O(\omega-\bar{\omega})$. Neglecting these terms yields the dispersion relation of the model of Lee et al. as

$$\frac{k}{\overline{k}} = \sqrt{1 + \frac{2\left(\frac{\omega}{\overline{\omega}}-1\right)}{\frac{\overline{C}_g}{\overline{C}} + \left(\frac{\omega}{\overline{\omega}}-1\right)\frac{\overline{k}^2}{\overline{\omega}}\overline{\frac{\partial}{\partial\omega}\left(CC_g\right)}}} \tag{14}$$

Substituting Eq. (12) into Eq. (4) of Lee et al., the imaginary part gives the energy transport equation given by

$$\nabla\cdot\left\{k\left[\overline{C}\overline{C}_g + (\omega-\overline{\omega})\overline{\frac{\partial}{\partial\omega}\left(CC_g\right)}\right]a^2\right\} = 0 \tag{15}$$

The shoaling coefficient is obtained from Eq. (15) as

$$K_s = \frac{a}{a_0} = \sqrt{\frac{k_0\left\{\left(\overline{C}\overline{C}_g\right)_0 + (\omega-\overline{\omega})\overline{\frac{\partial}{\partial\omega}\left(CC_g\right)_0}\right\}}{k\left\{\overline{C}\overline{C}_g + (\omega-\overline{\omega})\overline{\frac{\partial}{\partial\omega}\left(CC_g\right)}\right\}}} \tag{16}$$

where the wave number k is determined by the eikonal Eq. (13). For monochromatic waves, the shoaling coefficient of the model of Lee et al. is equal to the shoaling coefficient of the linear Stokes waves. For random waves with a local angular frequency different from the carrier one, the shoaling coefficient of the model of Lee et al. is approximate to an accuracy of $O(\omega-\bar{\omega})$.

In conclusion, for random waves, the linear dispersion of the model of Suh et al. is approximate to an accuracy of $O(\omega-\bar{\omega})$. However, other effects such as wave diffraction and higher-order bottom variations are considered only for monochromatic waves, and the shoaling coefficient of the model is approximate to an accuracy of less than $O(\omega-\bar{\omega})$. On the other hand, in the model of Lee et al., all of the dispersion relations, the effects of wave diffraction and higher-order bottom variations, and shoaling coefficient are approximate to an accuracy of $O(\omega-\bar{\omega})$. The dispersion relations of the two models have been compared against the exact solution in detail by Lee et al.

(2003). Therefore, only shoaling and diffraction are compared in the following section.

3. Numerical experiments

To test the applicability of the extended mild-slope equations of Suh et al. (1997) and Lee et al. (2003), we conducted numerical experiments for various cases. First, the two models were tested to simulate the shoaling of random waves over a planar slope. The shoaling spectra calculated by the models were compared against the spectra calculated by the shoaling coefficient of linear Stokes waves. Second, the two models were tested to simulate the diffraction of random waves through a breakwater gap on a flat bottom. The two numerical solutions were compared against the analytical solutions of Penney and Price (1952).

3.1. Numerical methods

We adopted a source function method of Wei et al. (1999) to generate waves. Sponge layers were placed at the outside boundaries to remove wave reflection from the boundaries by dissipating wave energy inside the sponge layers. Therefore, Eqs. (1) and (2) of Suh et al. are modified to

$$\frac{\partial \eta}{\partial t} = -\nabla\cdot\left(\frac{\overline{CC}_g}{g}\nabla\tilde{\phi}\right) + \frac{\overline{\omega}^2 - \overline{k}^2\overline{CC}_g}{g}\tilde{\phi} + \frac{\overline{\omega}^2}{g}\left\{\overline{R}_1(\nabla h)^2 + \overline{R}_2\nabla^2 h\right\}\tilde{\phi} + f_s(x,y,t) \tag{17}$$

$$\frac{\partial \tilde{\phi}}{\partial t} = -g\eta - \overline{\omega}D\tilde{\phi} \tag{18}$$

where $f_s(x,y,t)$ is a source function for the model of Suh et al. and the damping coefficient D is given by

$$D = \begin{cases} 0, & \text{outside sponge layer} \\ \dfrac{\exp(d/S)-1}{\exp(1)-1}, & \text{inside sponge layer} \end{cases} \tag{19}$$

where d is the distance from the starting point of the sponge layer and S is the thickness of the sponge layer. On the other hand, Eq. (4) of Lee et al. is modified to

$$\nabla\cdot\left(\overline{CC}_g\nabla\hat{\eta}\right) + \left\{\overline{k}^2\overline{CC}_g + g\overline{u}_1\nabla^2 h + g\overline{u}_2(\nabla h)^2\right\}\left(1+i\frac{D}{\overline{n}}\right)\hat{\eta} + i\nabla\cdot\left\{\overline{\frac{\partial(CC_g)}{\partial\omega}}\nabla\frac{\partial\hat{\eta}}{\partial t}\right\} + i\left\{\overline{\frac{\partial(k^2CC_g)}{\partial\omega}} + g\overline{\frac{\partial u_1}{\partial\omega}}\nabla^2 h + g\overline{\frac{\partial u_2}{\partial\omega}}(\nabla h)^2\right\}\left(1+i\frac{D}{\overline{n}}\right)\frac{\partial\hat{\eta}}{\partial t} = f_L(x,y,t) \tag{20}$$

where $f_L(x,y,t)$ is a source function for the model of Lee et al. and $\bar{n}=\bar{C}_g/\bar{C}$. The use of the source function method in the models of Suh et al. and Lee et al. is explained in detail in Kim et al. (2004).

The time derivative terms of the modified Eqs. (17) and (18) of Suh et al. are discretized by the Adams–Moulton predictor–corrector method (Kirby et al., 1992). The spatial derivative terms in the equations are discretized by a three-point symmetric formula. The modified Eq. (20) of Lee et al. is numerically solved by the Crank–Nicolson method in a horizontally one-dimensional domain and by the finite element method in a horizontally two-dimensional domain.

Initially, surface elevations are set to zero. In order to generate waves gradually, the source function is multiplied by $\tanh(t/p\bar{T})$, where $\bar{T}$ is the carrier wave period and p is a parameter corresponding to the rate of slow wave generation. Since the sponge layer reduces the incoming wave energy effectively, the reflective condition at the boundaries can be used.

3.2. Shoaling of random waves over a planar slope

To test the shoaling of random waves calculated by the two models, we simulated random waves shoaling over a plane with the slope of 1:100. The computational domain is shown in Fig. 1. The shoaling wave spectrum was obtained from the time series data of the surface elevation at a point on the shallow flat region. The TMA shallow-water spectrum was used as a target spectrum:

$$S(f) = \alpha g^2(2\pi)^{-4}f^{-5}\exp\left[-1.25\left(f/f_p\right)^{-4}\right]\gamma^{\exp\left[-\left(f/f_p-1\right)^2/2\sigma^2\right]} \times \phi_k(f,h) \tag{21}$$

where α is a spectral parameter, f_p is the peak frequency, γ is the peak enhancement factor, σ is the spectral width parameter ($\sigma=\sigma_a$ if $f\le f_p$ and $\sigma=\sigma_b$ if $f>f_p$, $\sigma_a=0.07$ and $\sigma_b=0.09$ were used), and finally the Kitaigordskii shape function, $\phi_k(f,h)$ incorporates the effect of the finite water depth as

$$\phi_k(f,h) = \begin{cases} 0.5\omega_h^2, & \omega_h < 1 \\ 1-0.5(2-\omega_h)^2, & 1\le\omega_h\le 2 \\ 1, & \omega_h > 2 \end{cases} \tag{22}$$

where $\omega_h = 2\pi f(h/g)^{1/2}$. In this study, $\alpha = 7.57\times10^{-4}$, $f_p = 0.767$ Hz, and $\gamma = 2$ were used. The frequency range was confined between 0.6 and 1.4 Hz so that the weighted-average frequency was 0.929 Hz.

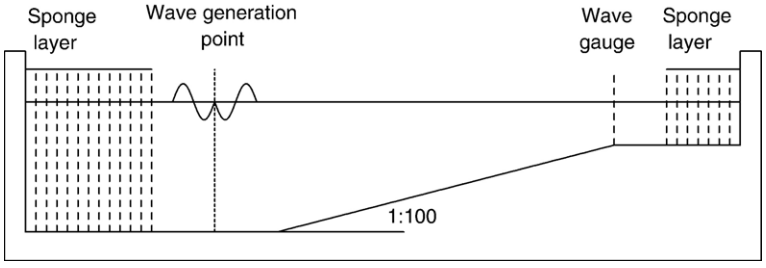

Fig. 1. Computational domain for shoaling test.

For the model of Suh et al., the peak frequency should be selected as a carrier frequency rather than the weighted-average frequency. The peak frequency is usually lower than the weighted-average one. And, the dispersion relation of the model of Suh et al. is accurate in the high frequency range regardless of the relative depth (Lee et al., 2003). For the model of Lee et al., however, it is better to use the weighted-average frequency as a carrier frequency. One reason is that, at lower frequencies, where the energy density is significant, the dispersion relation is accurate unless the frequency is too small. The other reason is that the model of Lee et al. may produce waves shorter than the exact ones in the higher frequency range and thus a smaller grid size is required for the solution, leading to increased computational costs and data storage requirements. This problem can be overcome by selecting the weighted-average frequency as a carrier frequency and by cutting off the higher frequency range where the wave energy is relatively small.

Numerical tests were conducted with the better carrier frequency of each model. With the peak frequency, which is the carrier frequency for the model of Suh et al., the relative water depth was 2π on the deep flat side and 0.1π on the shallow side. With the weighted-average frequency, which is the carrier frequency for the model of Lee et al., the relative water depth was 2.98π on the deep side and 0.12π on the shallow side.

Figs. 2 and 3 show comparisons of the shoaling wave spectra of the models against the exact solution. The input spectrum is also shown in the figures. The shoaling wave spectrum by the model of Lee et al. is closer to the exact one than that by the model of Suh et al. This is because the shoaling coefficient of the model of Lee et al. given by Eq. (16) takes into account the random wave characteristics to $O(\omega-\bar{\omega})$ but the shoaling coefficient of the model of Suh et al. given by Eq. (11) does not consider them properly. Such an inaccuracy of the model of Suh et al. in predicting shoaling of random waves may be attributed to the fact that the model was developed for a monochromatic wave even though the model's dispersion relation shows applicability to random waves.

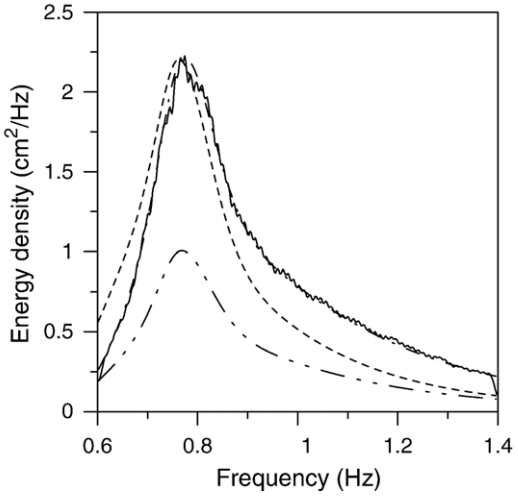

Fig. 2. Input spectrum and shoaling spectra calculated by the model of Suh et al.; dashed line = exact solution, solid line = numerical solution of the model of Suh et al., dash-dotted line = analytic solution of the model of Lee et al., dash-double-dotted line = input spectrum.

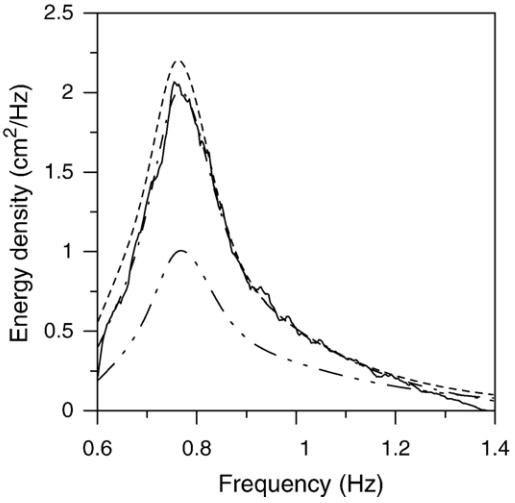

Fig. 3. Input spectrum and shoaling spectra calculated by the model of Lee et al.; dashed line = exact solution, solid line = numerical solution of the model of Lee et al., dash-dotted line = analytic solution of the model of Lee et al., dash-double-dotted line = input spectrum.

The models' significant wave heights at a certain water depth were calculated as

$$H_s = 4.004\sqrt{\int S_s(f,h)df} \tag{23}$$

where the shoaling spectrum $S_s(f,h)$ was calculated by multiplying the input spectrum by the square of the shoaling coefficient, which is given as Eqs. (11) or (16). Fig. 4 shows a comparison between the percent relative errors of the models' significant wave heights. As the relative water depth becomes smaller, the error of the model of Suh et al. becomes larger than that of the model of Lee et al. All the relative errors are less than 8% in the entire water depth. Note that the model of Suh et al. does not yield serious errors even though the model fails to accurately predict shoaling spectra of

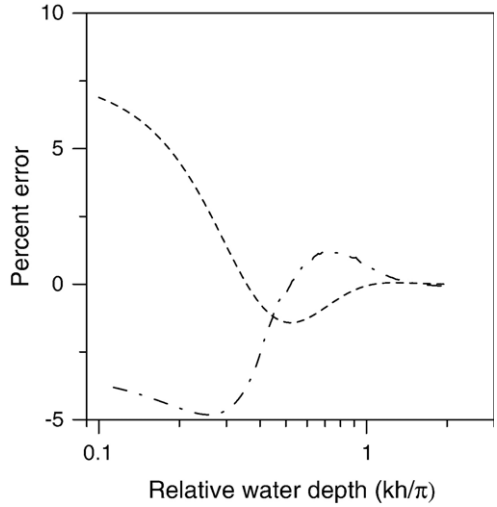

Fig. 4. Relative errors of significant wave heights of shoaling random waves; dashed line = model of Suh et al., dash-dotted line = model of Lee et al.

random waves. The reason can be found by looking at the shoaling spectra shown in Fig. 2. At frequencies lower than the peak, the model's spectrum is underestimated. However, at the higher frequencies, the model's spectrum is overestimated. Therefore, the significant wave heights of the model of Suh et al., which include all the solutions in whole frequency range, are not so different from the exact heights. This lucky coincidence may not defend the model of Suh et al. The wave-related phenomena such as wave–structure interaction and beach processes are analyzed more accurately based on the spectral calculation method rather than the significant wave representation. In this viewpoint, for random waves on varying topography, the use of the model of Lee et al. is more appropriate than the model of Suh et al.

3.3. Diffraction of random waves through a breakwater gap on a flat bottom

To test the diffraction of random waves, we simulated random waves propagating to a breakwater gap on a flat bottom. A part of the incident waves propagating directly on the breakwater was reflected from the structure while the remainder passed through the breakwater gap. The diffraction of waves may be seen between the geometric shadow and illuminated zones in the down-wave region of the breakwater. The diffraction theory for a large gap was developed by Penney and Price (1952). They showed that the Sommerfeld solution of the diffraction of light is also a solution of the water wave diffraction phenomenon. And, they concluded from a mathematical analysis that superposition of the solutions for each breakwater gives a good approximation as long as the width of the breakwater gap is greater than one wavelength.

The water depth is $h=1$ m and the period of the carrier wave is $\bar{T}=2.33$ s so that the relative water depth corresponding to the carrier wave is $\bar{k}h=0.313\pi$. The dispersion relations of the models of Suh et al. and Lee et al. are given by Eqs. (9) and (14), respectively. The exact dispersion relation for linear waves is given by

$$\frac{k}{\bar{k}}=\left(\frac{\omega}{\bar{\omega}}\right)^2\frac{\tanh \bar{k}h}{\tanh kh} \tag{24}$$

In this case, a comparison of the dispersion relation of each model against the exact one is shown in Fig. 5.

The length of the domain behind the breakwater is $10\bar{L}$ in both the x- and y-directions, where $\bar{L}=6.39$ m. The width of the breakwater gap is $B=2\bar{L}$ ($x=0$, $4\bar{L}\le y\le 6\bar{L}$). Waves are generated with the period of $T=3.88$ s on a line of $0.5\bar{L}$ up-wave of the breakwater. See the computational domain shown in Fig. 6.

The ratio of the local angular wave frequency to the carrier one is $\omega/\bar{\omega}=0.6$. In this case, the wavelengths determined by the linear Stokes waves, the model of Suh et al., and the model of Lee et al. are $L=11.61$, 15.02, and 12.13 m, respectively. That is, the wavelength by the model of Suh et al. is 29%

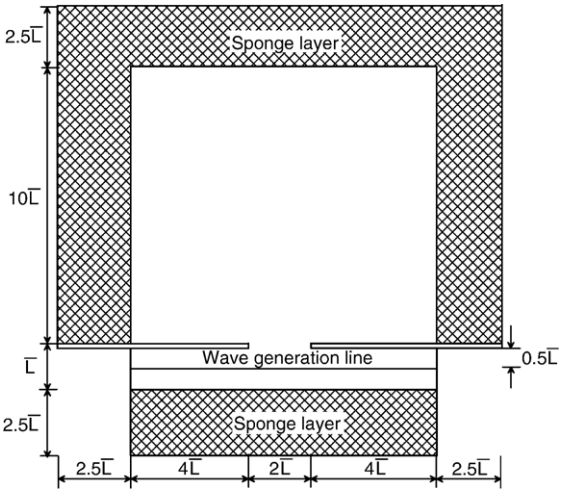

Fig. 6. Computational domain for diffraction test.

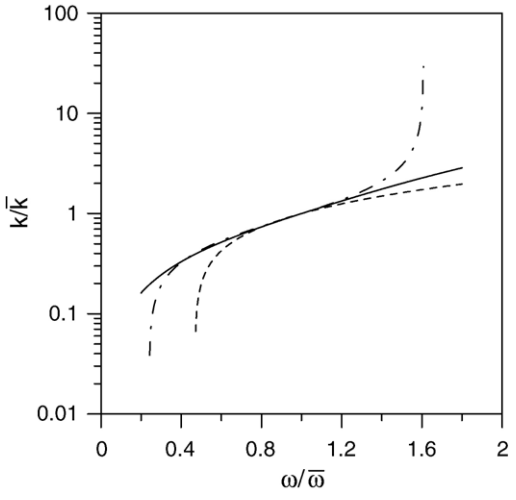

Fig. 5. Comparison of dispersion relations with best carrier frequencies in the diffraction test; solid line = linear Stokes waves ($\bar{k}h=0.313\pi$), dashed line = model of Suh et al. with a peak frequency ($\bar{k}h=0.313\pi$), dash-dotted line = model of Lee et al. with a weight-averaged frequency ($\bar{k}h=0.438\pi$).

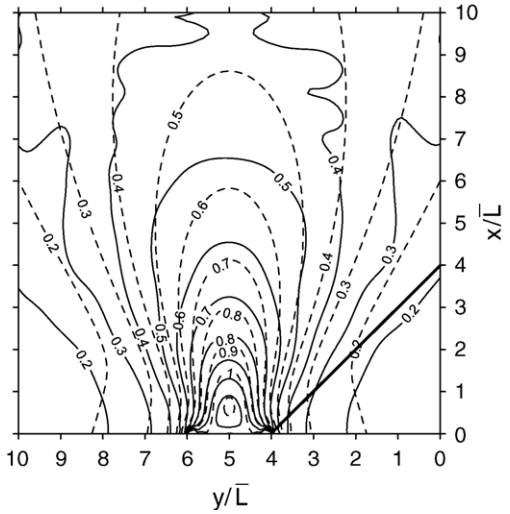

Fig. 7. Comparison of diffraction coefficients calculated by the model of Suh et al. against the exact solutions; solid line = numerical solution, dashed line = exact solution.

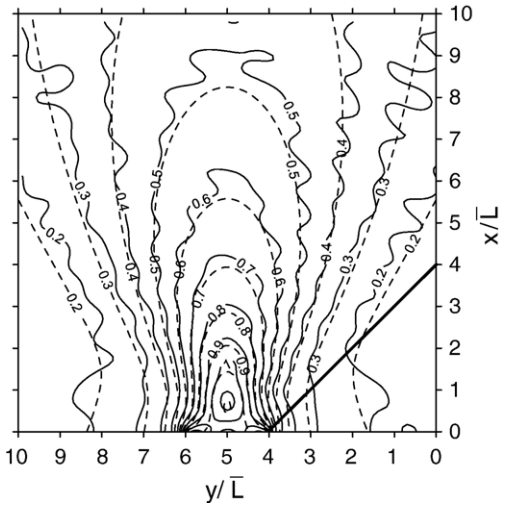

Fig. 8. Comparison of diffraction coefficients calculated by the model of Lee et al. against the exact solutions; solid line = numerical solution, dashed line = exact solution.

longer than the exact one, while the wavelength by the model of Lee et al. is only 4% longer. Therefore, the width of the gap, $B=2\bar{L}$, is seen as $B=1.10L$, $0.85L$, and $1.05L$, respectively, by the linear Stokes waves, the model of Suh et al., and the model of Lee et al.

Figs. 7 and 8 show comparisons of numerical solutions of the diffraction coefficient against the exact solution for the model of Suh et al. and the model of Lee et al., respectively. The model of Lee et al. yields more accurate solutions of the diffraction coefficient than the model of Suh et al. This is because, in the model of Lee et al., the linear dispersion relation gives more accurate solution for this case and furthermore the effects of random wave diffraction are approximate to an accuracy of $O(\omega-\bar{\omega})$. However, in the model of Suh et al., the effects of random wave diffraction are approximate to an accuracy of less than $O(\omega-\bar{\omega})$. It should be noted that the accuracy of the dispersion relation of each model depends on the relative water depth and the ratio of local to carrier frequencies. In the solution of the model of Suh et al., the gap width is seen to be narrower than in the solution of Lee et al. and thus the diffraction coefficients are more concentric from the central point of the gap. The diffraction coefficients along a line from ($x=0$, $y=4\bar{L}$) to ($x=4\bar{L}$, $y=0$) are larger in the model solution of Suh et al. than in the solution of Lee et al. This is because, compared to the model of Lee et al., the wavelength determined by the model of Suh et al. is longer, and the distance at a certain point from the tip of the breakwater is seen shorter, and thus the diffraction coefficients become larger. In conclusion, the diffraction coefficients of random waves are related dominantly to the dispersion relation of each model.

4. Conclusion

The extended mild-slope equations of Suh et al. (1997) and Lee et al. (2003) for random wave transformation were compared by both analytical methods and numerical simulations.

Using the method of geometric optics, the eikonal equation and energy transport equation for each model were obtained analytically. It was found from the eikonal equation that, in the model of Suh et al., the diffraction effects and higher-order bottom effects are considered only for monochromatic waves. It was found from the energy transport equation that the shoaling coefficient of the model of Suh et al. is not approximated with good accuracy. This inaccuracy comes from the fact that the model of Suh et al. was developed for regular waves. Luckily, even with the assumption of regular waves, the wave number was approximated with an accuracy of $O(\omega-\bar{\omega})$ at a constant water depth. In the model of Lee et al., however, all the parameters such as the wave number, the shoaling coefficient, diffraction effects, and higher-order bottom effects were approximated with an accuracy of $O(\omega-\bar{\omega})$. This is because the model of Lee et al. was developed using the Taylor series expansion technique for waves with local frequencies different from the carrier frequency.

The better carrier frequency for each model was chosen in view of the accuracy of the model's dispersion. For the model of Suh et al., the frequency was chosen as the carrier frequency. For the model of Lee et al., the weighted-average frequency, which is higher than the peak frequency, was chosen as the carrier frequency. Using the two models, we conducted numerical experiments to simulate the shoaling of random waves over a planar slope. The better carrier frequencies were selected for each model. The numerical solutions of shoaling spectra by the model of Lee et al. are more accurate than those by the model of Suh et al. Finally, numerical experiments were conducted to simulate the diffraction of random wave at a constant water depth. Numerical solutions of the diffraction coefficient agreed with the analytical solutions to the accuracy of the model's dispersion relation.

Acknowledgement

This work was supported by the Basic Research Program of the Korea Science and Engineering Foundation (No.: R01-2003-000-10635-0).

References

Berkhoff, J.C.W., 1972. Computation of combined refraction–diffraction. Proc. 13th Coastal Eng. Conf.. ASCE, pp. 471–490.

Chamberlain, P.G., Porter, D., 1995. The modified mild-slope equation. J. Fluid Mech. 291, 393–407.

Chandrasekera, C.N., Cheung, K.F., 1997. Extended linear refraction–diffraction model. J. Waterw. Port Coast. Ocean Eng. 123, 280–296.

Copeland, G.J.M., 1985. A practical alternative to the mild-slope wave equation. Coast. Eng. 9, 125–149.

Kim, G., Lee, C., Suh, K.-D., 2004. Generation of incident random waves in numerical mild-slope equation models using a source function method. Proc. 2nd Int. Conf. on Asian Pacific Coasts, Makuhari.

Kirby, J.T., Lee, C., Rasmussen, C., 1992. Time-dependent solutions of the mild-slope wave equation. Proc. 23rd Int. Conf. on Coastal Eng. ASCE, pp. 391–404.

Kubo, Y., Kotake, Y., Isobe, M., Watanabe, A., 1992. Time-dependent mild slope equation for random waves. Proc. 23rd Int. Conf. on Coastal Eng. ASCE, pp. 419–431.

Lee, C., Kirby, J.T., 1994. Analytical comparison of time-dependent mild-slope equations. J. Korean Soc. Coast. Ocean Eng. 6, 389–396.

Lee, C., Suh, K.D., 1998. Internal generation of waves for time-dependent mild-slope equations. Coast. Eng. 34, 35–57.

Lee, C., Park, W.S., Cho, Y.-S., Suh, K.D., 1998. Hyperbolic mild-slope equations extended to account for rapidly varying topography. Coast. Eng. 34, 243–257.

Lee, C., Kim, G., Suh, K.D., 2003. Extended mild-slope equation for random waves. Coast. Eng. 48, 277–287.

Massel, S.R., 1993. Extended refraction–diffraction equation for surface waves. Coast. Eng. 19, 97–126.

Nishimura, H., Maruyama, K., Hirakuchi, H., 1983. Wave field analysis by finite difference method. Proc. 30th Japanese Conf. Coastal Eng, pp. 123–127. (in Japanese).

Penney, W.G., Price, A.T., 1952. The diffraction theory of sea waves by breakwaters, and the shelter afforded by breakwaters. Philos. Trans. R. Soc. Lond. Ser. A 244, 236–253.

Radder, A.C., Dingemans, M.W., 1985. Canonical equations for almost periodic, weakly nonlinear gravity waves. Wave Motion 7, 473–485.

Smith, R., Sprinks, T., 1975. Scattering of surface waves by a conical island. J. Fluid Mech. 72, 373–384.

Suh, K.D., Lee, C., Park, W.S., 1997. Time-dependent equations for wave propagation on rapidly varying topography. Coast. Eng. 32, 91–117.

Wei, G., Kirby, J.T., Sinha, A., 1999. Generation of waves in Boussinesq models using a source function method. Coast. Eng. 36, 271–299.